Protonation Processes and Electronic Spectra of Histidine and Related Ions

Zhijian Huang, Zijing Lin,* and Ce Song

Hefei National Laboratory for Physical Sciences at Microscale and Department of Physics, University of Science and Technology of China, Hefei, China 230026

Received: November 5, 2006; In Final Form: January 20, 2007

A full structural assignment of the neutral, protonated, and deprotonated histidine conformers in the gas phase is presented. A total of 3024 unique trial structures were generated by all combinations of internal single-bond rotamers of these species and optimized at the B3LYP/6-311G* level and further optimized at the B3LYP/6-311++G** level. A set of unique conformers is found, and their relative energies, free energies, dipole moments, rotational constants, electron affinities, ionization energies, and harmonic frequencies are determined. The population ratio of histidine and its tautomer is 1:0.16 at 298 K. Massive conformational changes are observed due to protonation and deprotonation, and the intramolecular H-bonds are characterized with the atoms in molecules theory. The calculated proton dissociation energy, gas-phase acidity, proton affinity, and gas-phase basicity are in excellent agreement with the experiments. The deprotonation and protonation of gaseous histidine both occur on the imidazole ring, explaining the versatile biofunctions of histidine in large biomolecules. The UV spectra of neutral and singly and doubly protonated histidine are investigated with the TDDFT/B3LYP/6-311+G(2df,p) calculations. The S_0-S_1, S_0-S_2, and S_0-S_3 excitations of histidine are mixed $\pi\pi^*/n\pi^*$ transitions at 5.37, 5.44, and 5.69 eV, respectively. The three excitation energies for histidine tautomer are 4.85, 5.47, and 5.52 eV, respectively. The three excitations for protonated histidine are mainly $n\pi^*$ transitions at 5.45, 5.67, and 5.82 eV, respectively. The S_0-S_1 excitation of protonated histidine produces $ImH-C_\beta H_2-C_\alpha H(COOH)-NH_2^+$, while the S_0-S_2 and S_0-S_3 transitions produce $ImH-C_\beta H_2-C_\alpha H(NH_2)-(COOH)^+$. These data may help to understand the mechanisms of the UV fragmentation of biomolecules.

1. Introduction

Histidine is one of the most versatile protein residues. Its imidazole side chain has a pK_a near neutrality and frequently serves as a general acid or base in catalysis and in ligation of essential metal ions.[1] This property is inherent neither to the standard nucleotides nor to the remaining natural amino acids. As a consequence, histidine is one of the residues most frequently used to form the active sites of protein enzymes. Even though the value of studying isolated molecules is affected by the neglect of environmental influence, detailed knowledge of the structures and properties of histidine and the related molecules is important for our understanding of their static and dynamic properties in larger biosystems. Indeed, we will demonstrate in this contribution that both the deprotonation and protonation processes of gaseous histidine molecule occur on the imidazole ring, and the effect of peptide chain formation should be inconsequential.

The biological function of a molecule is often intimately dependent upon the conformations that the molecule adopts.[2] The imidazole side chain of free neutral histidine may exist in two forms: the $N^\epsilon-H$ tautomer, His[N^ϵH], and the $N^\delta-H$ tautomer, His[N^δH] (see Scheme 1). The equilibrium between these two forms generally exists at high pH. Histidine takes the preferential conformation of His[N^ϵH] in natural protein and other biological molecules. In protonated canonical histidine, one proton may be attached to two alternative sites, namely, the amine group and the imidazole side chain, forming cationic species $HisH^+[NH_2]$ and $HisH^+[N^\delta]$, respectively. Doubly protonated histidine has only one tautomeric form, denoted as $HisH_2^{2+}$. Similarly, a proton can be detached on two possible sites, forming anionic species His^-[COOH] and $His^-[N^\epsilon H]$, respectively, corresponding to deprotonation sites of the carboxyl group and the imidazole side chain. Doubly deprotonated histidine, His^{2-}, has only one tautomeric form. The possible protonation/deprotonation processes of gaseous histidine are sketched in Scheme 1. The protonation/deprotonation processes of gaseous histidine are not clearly known yet, but can be identified by accurate first-principle calculations of proton affinity (PA), gas-phase basicity (GB), proton dissociation energy (PDE), and gas-phase acidity (GA) of the possible protonation/deprotonation processes in comparison with the experimental data.

The acid−base properties of a biomolecule affect physicochemical activities such as solubility, hydrophobicity, and electrostatic interactions which directly impact the biological activity of the molecule in a living system. Many biochemical processes carry out the message transferred by proton-transfer reaction. The rate of reaction is directly related to the special acidity/basicity of the biomolecular compound. The PA and GB of the protonation reaction and PDE and the GA of the deprotonation reaction are fundamental properties essential for a quantitative understanding of the intrinsic properties of a peptide in the absence of solvents. Several experiments have been dedicated to provide accurate measurements of these chemical properties for amino acids.[3−7] Theoretical calculations[8−19] have also provided the gas-phase conformational information and thermodynamics parameters that relate the experimental GB

* To whom correspondence should be addressed. Telephone: +86-551-3606345. Fax: +86-551-3606348. E-mail: zjlin@ustc.edu.cn.

10.1021/jp067280a CCC: $37.00
Published on Web 05/03/2007

SCHEME 1: Reaction Paths for Protonation and Deprotonation of Histidine in the Gas Phase

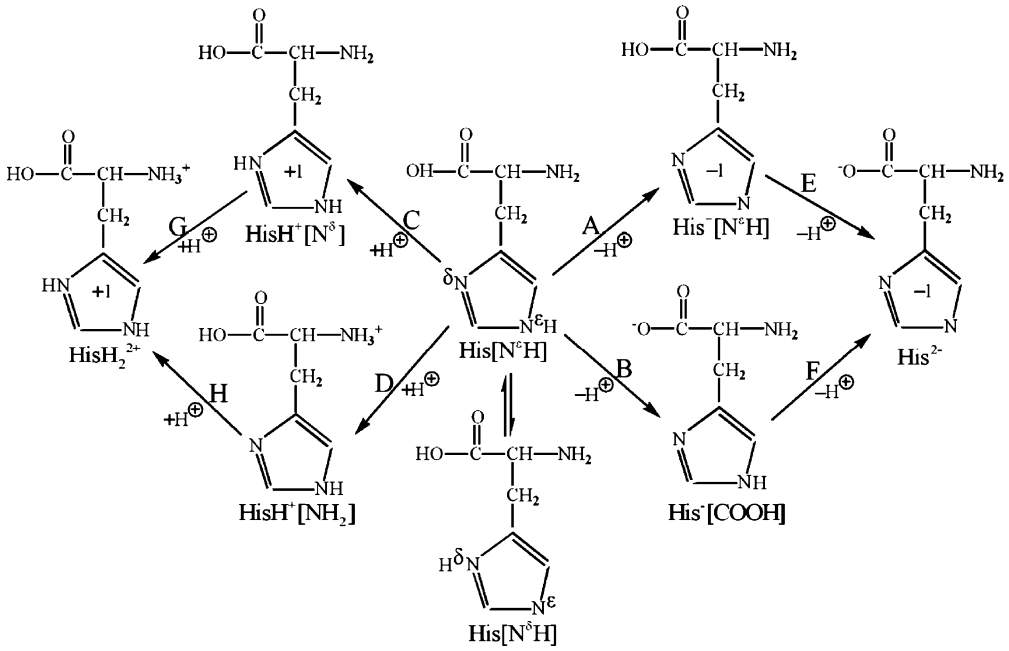

SCHEME 2: Schematic Illustration of the Degrees of Freedom of Rotamers of Neutral, Deprotonated, and Protonated Histidine[a]

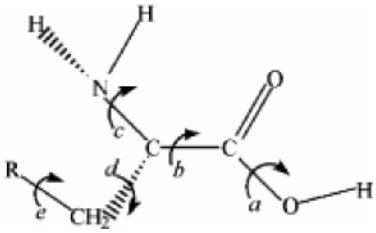

[a] (a) 2-fold: 0, 180 (except His^-[COOH] and His^{2-}). (b) 6-fold: 30, 90, 150, 210, 270, 330. (c) 3-fold: −120, 0, 120 (except $HisH^+[NH_2]$ and $HisH_2^{2+}$). (d) 6-fold: −120, −60, 0, 60, 120, 180. (e) 3-fold : 60, 120, 180.

and PA in a protonation reaction.[11,20−21] As a proton transfer is usually coupled with a conformational change,[16−19] thorough conformational searches of the neutral, protonated, and deprotonated histidines need to be performed in order to obtain accurate computational results of the thermodynamics properties.[22]

Here we performed intensive computations to locate all the stable conformers of the tautomeric, deprotonated, and protonated histidines. The intramolecular H-bonding properties of the tautomeric, deprotonated, and protonated histidine conformers were characterized in detail using the atoms in molecules (AIM) theory.[23,24] The PDE, PA, GA, and GB of canonical neutral histidine were calculated and compared with the experimental data[7,25] to unravel the protonation and deprotonation processes of gaseous histidine.

The rich photophysics of DNA bases due to numerous n, π, and σ electrons is very important since the ultraviolet (UV) spectra and the excited-state lifetimes control the crucial questions of radiation-induced damages in DNA and the possible occurrence of undesired photochemical effects. Laser-based techniques combined with supersonic jets now allow experimentalists to distinguish the contribution of different tautomers as well as to measure their intrinsic photophysical features. The main features of the near- and far-ultraviolet spectra of proteins are related to the absorption properties of the aromatic amino acids[26,27] and thus have been the subject of most laser spectroscopic studies on amino acids so far.[28−36] It is found that the peptide or the amide chromophores absorb in the region of 220 to 190 nm (5.64−6.53 eV), and tyrosine and tryptophan absorption occurs in the region around 280 nm (4.43 eV).[27] The excited states of neutral and protonated tryptohan have been calculated by time-dependent density functional theory (TD-DFT)[33,34] and are in good agreement with the experiments. Resonance enhancement of imidazole vibrations is weak, and histidine UV resonance Raman (UVRR) bands are usually obscured by stronger signals from the rest of the protein. However, it has been possible to detect certain histidine signals when the imidazole is protonated[37] or bound to metal ions.[38,39]

The TDDFT method was used in this work to calculate the electronic spectra of gaseous histidine and related ions. The charge-transfer processes in the excitation transition of neutral and protonated histidine were revealed in detail.

2. Computational Method

The conformational spaces of histidine and its related ions were explored by allowing for all combinations of the internal single-bond rotators (see Scheme 2). The total numbers of trial structures thus generated for His[N^δH], $HisH^+[N^\delta]$, $HisH^+$-[NH_2], $His^-[N^\epsilon H]$, His^-[COOH], $HisH_2^{2+}$, and His^{2-} are 648, 648, 216, 648, 324, 216, and 324, respectively. These trial geometries were optimized at the B3LYP/6-311G(d) level, and a set of unique conformers were located. All stationary points were verified as local minima by frequency calculations, and the data from which were also used to compute thermal contributions to gas-phase enthalpies and Gibbs free energies using the standard ideal-gas, rigid-rotor, harmonic-oscillator partition-function approximations. To ascertain the structural accuracy and stability, all conformers obtained at the B3LYP/6-311G(d) level were further optimized at the B3LYP/6-311++G(d,p) level with no noticeable structural changes, consistent with the finding for neural canonical histidine His-[N^ϵH].[40] Single-point energy calculations were performed at the B3LYP/6-311+G(2df,p) and MP2/6-311+G(2df,p) levels of theory for all the found conformers. The vertical ionization

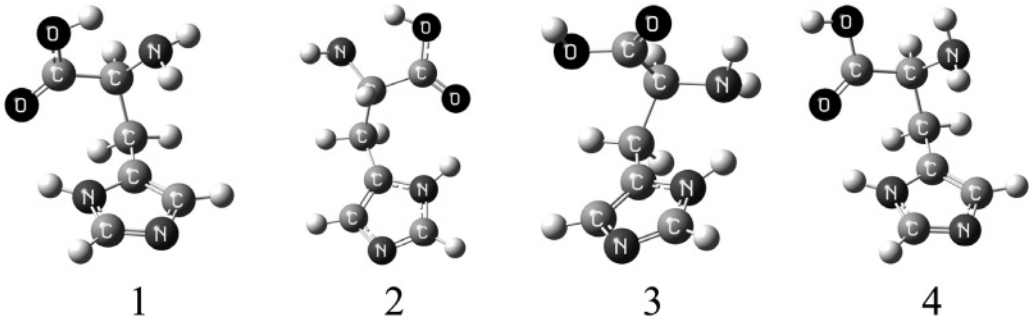

Figure 1. Structures of the four most stable conformers of tautomer histidine His[N$^{\delta}$H].

TABLE 1: Relative Electronic Energies, Enthalpies, Free Energies, Rotational Data, and Dipole Moments for the Four Most Stable Histidine Tautomeric Conformers in the Gas Phase[a]

	relative energy					rotational constants			
Conformer	B1	B2	M	relative enthalpy	relative free energy	A	B	C	dipole moment (D)
1	0.00	0.00	0.00	0.00	0.00	1.886	0.790	0.712	4.43
2	0.64	0.55	1.43	0.60	0.54	3.019	0.561	0.493	7.86
3	1.40	1.38	3.20	1.36	1.14	3.017	0.558	0.484	5.07
4	2.08	1.83	3.56	1.61	1.35	2.422	0.677	0.555	2.85

[a] Relative energies in kilocalories per mole at the B3LYP/6-311G* (B1), B3LYP/6-311+G(2df,p) (B2), and MP2/6-311+G(2df,p) (*M*) levels. Relative enthalpy and free energy at 298 K in kilocalories per mole are the B3LYP/6-311+G(2df,p) electronic energy plus the respective vibrational energy correction to enthalpy and free energy obtained at the B3LYP/6-311G* level. Rotational constants (GHz) and dipole moments (D) were obtained at the B3LYP/6-311+G(2df,p) level. Note that the vibrational frequencies were scaled by the factor 0.96.[52]

energies and electron affinities of histidine species were also computed at the B3LYP/6-311+G(2df,p) level. The B3LYP method was shown to provide accurate molecular structures and the associated vibrational spectra of amino acids[41,42] and applied in this study due to its high efficiency. The MP2 method was used in this work for comparison. All calculations were performed using the Gaussian 98 software package.[43]

Intramolecular hydrogen bonds of the canonical neutral, deprotonated, and protonated histidine conformers were analyzed with the AIM theory[44−46] based on the B3LYP/6-311+G(2df,p) densities. The hydrogen bond strength was characterized with a simple empirical relationship between the potential energy density at the bond critical point V_{cp} and the gross hydrogen bond energy E_{HB} as derived by Espionsa et al.,[47] $E_{HB} = {}^1/_2V_{cp}$. Notice that the expression for the H-bond energy disregards the energy cost of steric interaction of forming the H-bond and is larger than the net H-bond energies.[48] Nevertheless, the results are indicative of the relative H-bond strength.[49]

The thermodynamic properties of histidine and its related ions were calculated at the reference state of 1 atm and 298 K. Proton affinity (PA) was determined as the negative enthalpy change of protonation reaction C, D, G, or H (see Scheme 1). Gas-phase basicity corresponded to the negative Gibbs energy change of the protonation reaction. Proton dissociation energy was the enthalpy change of deprotonation reaction A, B, E, or F (see Scheme 1). Gas-phase acidity corresponded to the Gibbs free energy change of the deprotonation reaction. The enthalpy change was calculated as

$$\Delta H_r = \Delta E_e(0) + \Delta E_v(0) + \Delta(\Delta E_v(298)) + \frac{5}{2}RT$$

where $\Delta E_e(0)$ was the change of the total electronic energy, $\Delta E_v(0)$ the change in the zero point vibrational energy, $\Delta(\Delta E_v(298))$ the change of vibration energy during heating from 0 to 298 K, and ${}^5/_2RT$ the classic term accounting for the effect of losing three translational degrees of freedom. The Gibbs energy change was obtained as follows: $\Delta G = \Delta H - T\Delta S$. At 298 K, $TS(H^+) = 7.76$ kcal/mol and the enthalpy and Gibbs free energy of proton are 1.48 kcal/mol and −6.27 kcal/mol, respectively.

Each species of gaseous histidine and related ions is populated over a few conformers. The relative abundances of different conformers are determined by the differences in their free energies. The conformational equilibrium effect (CEE) should in general be considered in calculating the thermodynamic properties. This can be easily done with population averaging. For example, a population-averaged free energy may be calculated as $G^\circ = -RT \ln(\Sigma_i e^{-Gi^\circ/RT})$, where R is the universal gas constant, T is the absolute temperature (298.15 K), and i runs over all conformers.

The excited states of the canonical neutral histidine and related ions were calculated by the TDDFT/B3LYP/6-311+G(2df,p) method as the method gave results in good agreement with experiments as well as those by more sophisticated methods such as CASPT2.[33,50−51]

3. Results and Discussion

3.1. Conformations and Ground-State Properties of Histidine and Related Ions in the Gas Phase. *Canonical Neutral Histidine (His[N$^{\epsilon}$H] and His[N$^{\delta}$H]).* We focus here on the properties of histidine tautomer His[N$^{\delta}$H] as the properties of gaseous histidine His[N$^{\epsilon}$H] have been reported in detail before.[40] A total of 40 stable conformers of His[N$^{\delta}$H] were located. The 40 conformers span an energy range of 14 kcal/mol at the B3LYP/6-311+G(2df,p) level. As the hydrogen on the nitrogen in the imidazole ring may be near the backbone in His[N$^{\delta}$H] and form intramolecular H-bond with amino group and carboxylic group, the characteristics of the His[N$^{\delta}$H] conformers are somewhat different from those of His[N$^{\epsilon}$H]. Table 1 lists the relative energies, rotational constants, and dipole moments for the four most stable gaseous His[N$^{\delta}$H] conformers. The structures of the four most stable conformers are shown in Figure 1. The two most stable conformers, with the dipole moments of 4.43 and 7.86 D, respectively, are found to be stabilized by the intramolecular interaction of OH···NH$_2$ and N$^{\delta}$H···O=C H-bonds. At 298 K, the percent shares of the most stable and the second most stable conformers are respectively 65 and 10% of the total His[N$^{\delta}$H] population. The Gibbs free energy of the most stable His[N$^{\delta}$H] conformer is 1.1 kcal/mol higher than

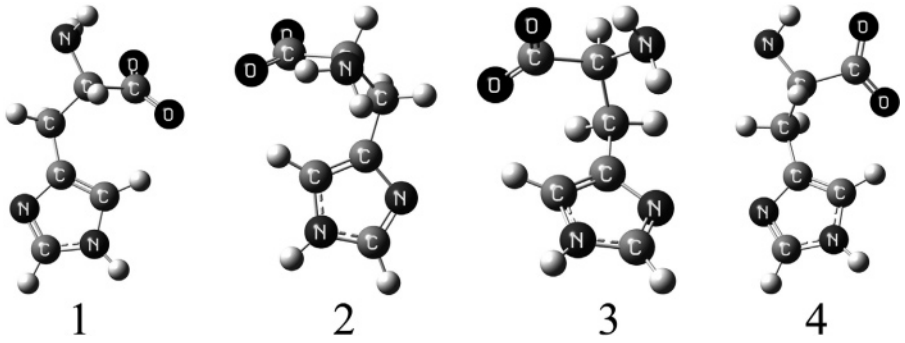

Figure 2. Structures of the four most stable conformers of deprotonated histidine His$^-$[COOH].

TABLE 2: Relative Electronic Energies, Enthalpies, Free Energies, Rotational Data, and Dipole Moments for the Four Most Stable Conformers of Deprotonated Histidine His$^-$[COOH] in the Gas Phase[a]

	relative energy					rotational constant			
conformer	B1	B2	M	relative enthalpy	relative free energy	A	B	C	dipole moment (D)
1	0.00	0.00	0.00	0.00	0.00	2.283	0.689	0.574	8.13
2	0.42	0.11	-1.04	0.19	0.22	2.074	0.739	0.697	9.37
3	0.45	0.13	-1.26	0.19	0.13	1.994	0.790	0.691	8.74
4	0.80	0.47	1.44	0.43	0.21	2.490	0.656	0.541	9.05

[a] See footnote *a* of Table 1.

TABLE 3: Relative Electronic Energies, Enthalpies, Free Energies, Rotational Data, and Dipole Moments for the Four Most Stable Conformers of Deprotonated Histidine His$^-$[N$^\epsilon$H] in the Gas Phase[a,b]

	relative energy					rotational constant			
conformer	B1	B2	M	relative enthalpy	relative free energy	A	B	C	dipole moment (D)
1	−7.93	−7.35	−11.43	−8.15	−7.50	2.491	0.726	0.652	3.17
2	−5.52	−3.83	−7.56	−3.73	−3.06	3.133	0.568	0.503	5.11
3	−3.41	−1.27	−4.55	−1.18	−0.62	3.158	0.564	0.490	5.40
4	−2.67	−1.12	−4.94	−1.16	−0.56	2.038	0.733	0.673	7.06

[a] The relevant energies of the most stable His$^-$[COOH] conformer are used as the references. [b] See footnote *a* of Table 1.

that of His[N$^\epsilon$H], corresponding to a tautomeric form ratio of 0.16. The tautomeric form ratio is similar to that by the experimental[53] and molecular dynamics estimates[54] for histidine in solution. Notice, however, the agreement is only coincidental as the tautomeric states of histidine in solutions, peptides,[55] or proteins[56] may have rather different relative energies. For example, the most stable tautomers of gaseous GlyHis and HisGly were found to be the N$^\delta$−H and N$^\epsilon$−H tautomers, respectively.[55]

According to the AIM analysis, seven types of H-bonds, OH···NH$_2$, N$^\delta$H···O═C, N$^\delta$H···OH, N$^\delta$H ··NH$_2$, CH$_r$···O═C (r denotes the imidazole ring), CH$_r$···OH, and OH···C$_r$, are identified in the 40 His[N$^\delta$H] conformers. Some of the H-bonds resemble that found in the *N*-formyl-L-histidinamide, where the N$^\delta$H group may act as a donor of H-bond to interact with the oxygen of the carbonyl group and the nitrogen of the amino group.[19] As in the case for phenylalanine,[32,57] CH$_r$ is found here to serve as an H-bond donor and interact with the oxygen of the carboxylic group.[57,58] The OH···NH$_2$ H-bond is moderately strong, with an average energy of −9.0 kcal/mol, similar to that found in His[N$^\epsilon$H] conformers.[40] Other H-bonds are relatively weak, and their average energies are as follows: E_{HB}(N$^\delta$H···O═C) = −3.9 kcal/mol, E_{HB}(N$^\delta$H···OH) = −2.6 kcal/mol, E_{HB}(N$^\delta$H···NH$_2$) = −3.5 kcal/mol, E_{HB}(CH$_r$···O═C) = −1.9 kcal/mol, E_{HB}(CH$_r$···OH) = −1.4 kcal/mol, and E_{HB}(OH···C$_r$) = −2.9 kcal/mol. Overall, the His[N$^\epsilon$H] tautomer has higher hydrogen bonding capabilities than that of the His[N$^\delta$H] tautomer.

Deprotonated Hisditine (His$^-$[COOH] and His$^-$[N$^\epsilon$H]). Detachment of a proton from the carboxylic group of histidine is denoted His$^-$[COOH]. On the potential energy surface, 12 conformers were found. Table 2 summarizes the relative energies, rotational data, and dipole moments for the four most stable His$^-$[COOH] conformers. The energies of the 12 conformers vary in the range of 4 kcal/mol at the B3LYP/6-311+G(2df,p) level. The AIM analysis of the 12 conformers identified three types of H-bond, NH···O, CH$_r$···O (see Figure 2), and CH$_r$···NH$_2$ (conformer 8, not shown). The average H-bond energies of NH···O, CH$_r$···O, and CH$_r$···NH$_2$ are, respectively, −6.1, −3.6, and −2.2 kcal/mol. The six most stable conformers have similar structures, containing both NH···O and CH$_r$···O H-bonds. Their energy gap is very small by about 1 kcal/mol. The three highest conformers only contain a NH···O H-bond. Notice that there is no NH···O H-bond in the neutral species.[40] The presence of the NH···O H-bond in His$^-$[COOH] is due to the increased electron denisty of oxygen in the anionic carboxyl group. The strength of CH$_r$···O also increases. The H-bond energy of CH$_r$···O in His$^-$[COOH] is higher than its counterpart in the neutral species by 1.5 kcal/mol or more.

When a proton is detached from the imidazole ring, the tautomer is denoted His$^-$[N$^\epsilon$H]. A set of 29 unique His$^-$[N$^\epsilon$H] conformers was located. The energies of the 29 conformers vary by about 20 kcal/mol at the B3LYP/6-311+G(2df,p) level. Table 3 shows the relative energies, rotational constants, and dipole moments for the four lowest-energy conformers. Four types of H-bonds (OH···N$^\delta$, OH···NH$_2$, NH··· N$^\delta$, and OH···C$_r$) were found on the basis of AIM theory. The N of imidazole ring is an excellent proton acceptor in the deprotonated tautomer His$^-$[N$^\epsilon$H]. The OH···N$^\delta$ bond is very strong and has an energy of −26.3 kcal/mol. The average H-bond energies of OH···NH$_2$, NH···N$^\delta$, and OH···C$_r$ are −11.3, −5.1, and −6.1 kcal/mol, respectively. The OH···NH$_2$ energy is slightly higher than that

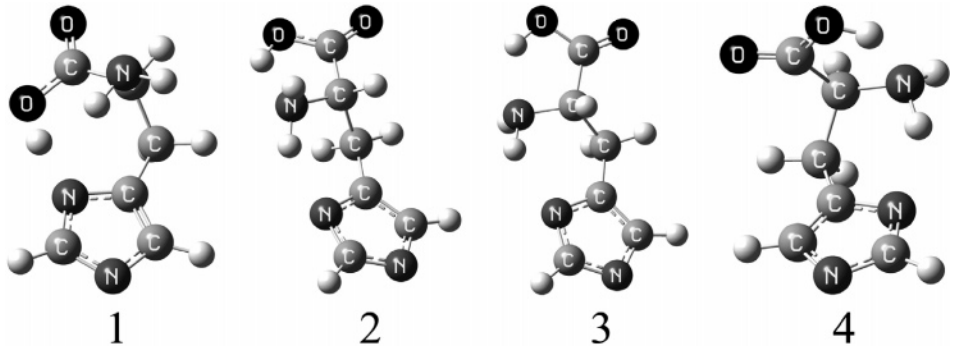

Figure 3. Structures of the four most stable conformers of deprotonated histidine $His^{-}[N^{\epsilon}H]$.

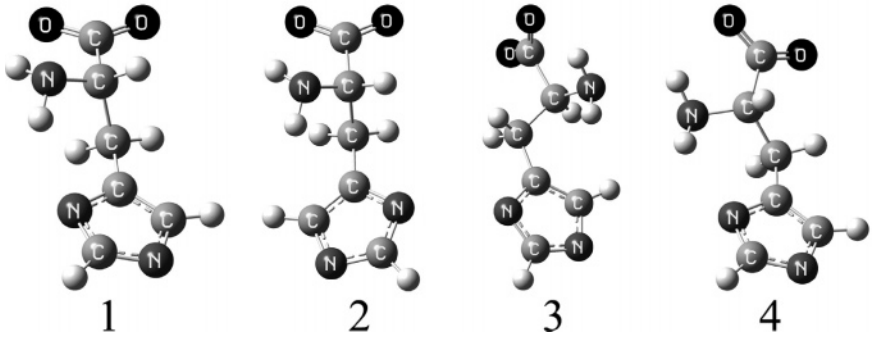

Figure 4. Structures of the four most stable conformers of histidine dianion His^{2-}.

TABLE 4: Relative Electronic Energies, Enthalpies, Free Energies, Rotational Data, and Dipole Moments for the Four Most Stable Conformers of Doubly Deprotonated Histidine in the Gas Phase[a]

	relative energy					rotational constant			
conformer	B1	B2	M	relative enthalpy	relative free energy	A	B	C	dipole moment (D)
1	0.00	0.00	0.00	0.00	0.00	3.084	0.555	0.496	2.82
2	1.41	0.71	0.55	0.57	0.32	3.075	0.546	0.505	2.99
3	2.12	1.23	1.17	1.13	0.66	3.092	0.532	0.506	2.38
4	3.35	3.20	3.67	2.95	2.78	3.081	0.554	0.485	2.91

[a] See footnote *a* of Table 1.

of neutral tautomers due to the cooperative interaction of H-bonds.[32] The most stable conformer is stabilized by the N of the imidazole ring simultaneously interacting with the amino group and hydroxyl group (see Figure 3). Conformers 2−4 are stabilized by the OH···NH_2, NH··· N_r H-bonds. The most stable conformer of $His^{-}[N^{\epsilon}H]$ is more stable than its His^{-}[COOH] counterpart by 7.5 kcal/mol in the free energy scale. Therefore, the His^{-}[COOH] tautomers can be ignored in the gas phase. There is also a big free energy gap (4.4 kcal/mol) between the most and the second most stable conformers of $His^{-}[N^{\epsilon}H]$, and the most stable $His^{-}[N^{\epsilon}H]$ conformer can be viewed as the sole equilibrium structure at 298 K.

Doubly Deprotonated Histidine (His^{2-}). Deprotonation of the second proton from the remaining possible losing site plays a vital role in biological functions of histidine in the peptides and proteins. A total of 10 conformers was found. The relative energies, rotational constants, dipole moments, and thermodynamic data of the four most stable conformers are listed in Table 4. The energy span of the 10 conformers is about 9.5 kcal/mol at the B3LYP/6-311+G(2df,p) level.

Only two types of H-bond, NH···O and NH···N^{δ}, were found in the 10 conformers by the AIM analysis. The average strengths of NH···O and NH···N^{δ} bonds are −6.9 and −2.4 kcal/mol, respectively. The structures of the six most stable conformers are similar, with the anionic carboxyl group deviating away from the imidazole ring and the amino group lying in the middle to interact with the two groups and forming a NH···O H-bond (Figure 4). From Table 4, the dipole moments of dianionic forms are much lower than those of anionic forms. Such configuration helps to reduce the electron repulsion and increase the conformational stability. When the two negative charges are close to each other as in conformers 7−10 (not shown), the energy of the conformer increases and the structure is disfavored.

Protonated Histidine ($HisH^{+}[NH_2]$ and $HisH^{+}[N^{\delta}]$). Both the amino group and imidazole ring can provide protonated sites in the canonical neutral histidine. Protonation of $His[N^{\epsilon}H]$ or $His[N^{\delta}H]$ produces the same most important protonation tautomers, and we focus here on the protonation of $His[N^{\epsilon}H]$ due to its high abundance. Attachment of the proton to the amino group forms the tautomeric species $HisH^{+}[NH_2]$. After optimizations of all possible trial structures, 11 stable conformers were located. The energies of the 11 conformers vary by about 20 kcal/mol at the B3LYP/6-311+G(2df,p) level. Table 5 summarizes the relative energies, rotational constants, dipole moments, and thermodynamic data for the four most stable conformers. The ammonium after protonating the amino group can serve as a strong donor of H-bond due to its positive electronic charge but cannot act as an acceptor of a H-bond. Three types of strong H-bond (NH_3^{+}···N^{δ}, NH_3^{+}···O═C, and OH···N^{δ}) were identified by the AIM analysis. The average energies of H-bonds are $E_{HB}(NH_3^{+}\cdots N^{\delta}) = -15.6$ kcal/mol, $E_{HB}(NH_3^{+}\cdots O{=}C) = -10.3$ kcal/mol, and $E_{HB}(OH\cdots N^{\delta}) = -22.4$ kcal/mol, respectively. In the four most stable conformers, the ammonium lies between the *trans*-carboxyl group and the

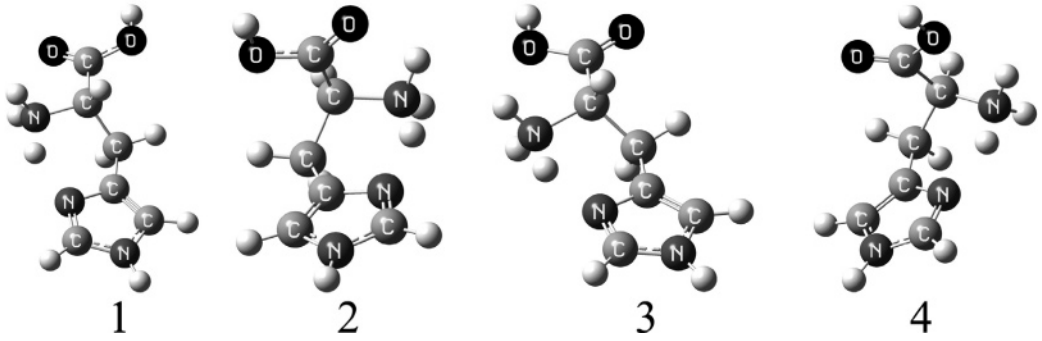

Figure 5. Structures of the four most stable conformers of protonated histidine $HisH^+[NH_2]$.

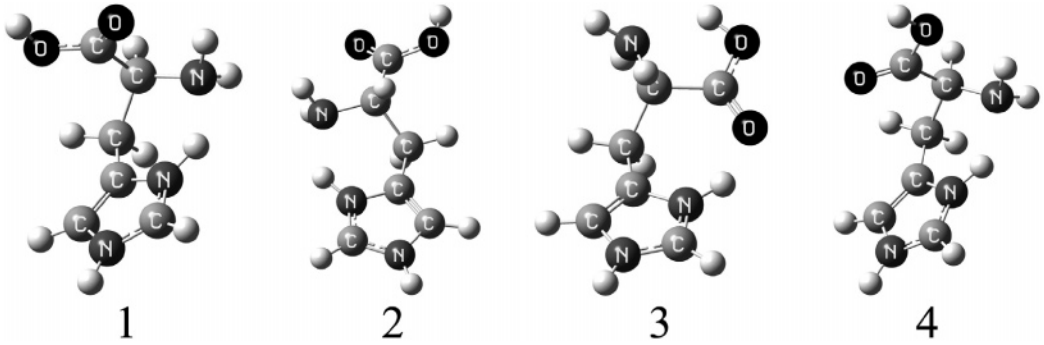

Figure 6. Structures of the four most stable conformers of protonated histidine $HisH^+[N^\delta]$.

TABLE 5: Relative Electronic Energies, Enthalpies, Free Energies, Rotational Data, and Dipole Moments for the Four Most Stable Conformers of Protonated Histidine $HisH^+[NH_2]$ in the Gas Phase[a]

	relative energy					rotational constant			
conformer	B1	B2	M	relative enthalpy	relative free energy	A	B	C	dipole moment (D)
1	0.00	0.00	0.00	0.00	0.00	3.029	0.563	0.493	2.68
2	0.21	0.27	-0.49	0.20	0.47	1.907	0.765	0.707	2.16
3	2.48	3.07	2.97	3.00	2.80	3.077	0.562	0.486	4.09
4	2.55	3.13	2.15	2.99	3.15	1.925	0.759	0.710	3.96

[a] See footnote *a* of Table 1.

TABLE 6: Relative Electronic Energies, Enthalpies, Free Energies, Rotational Data, and Dipole Moments for the Four Most Stable Conformers of Protonated Histidine $HisH^+[N^\delta]$ in the Gas Phase[a,b]

	relative energy					rotational constant			
conformer	B1	B2	M	relative enthalpy	relative free energy	A	B	C	dipole moment (D)
1	−0.51	−1.69	−0.54	−2.07	−2.10	1.880	0.772	0.721	5.88
2	−0.53	−1.53	0.64	−1.81	−1.95	3.007	0.559	0.490	8.33
3	1.22	−1.32	2.13	−1.72	−1.16	2.468	0.666	0.541	8.36
4	0.23	−0.90	0.16	−1.18	−1.10	2.021	0.751	0.704	5.40

[a] The energies of the most stable $HisH^+[NH_2]$ conformer are used as the references. [b] See footnote *a* of Table 1.

imidazole ring (Figure 5). As found in the protonated glycine,[14,17] serine,[17] cysteine,[17] and tryptophan,[34] the most stable conformation shows an intramolecular hydrogen bond between NH_3^+ and the carboxylic oxygen and a favorable interaction between NH_3^+ and the side chain. When the carboxyl group lies between the ammonium and imidzole ring with the positive charge exposed on the molecular external surface, the energy of the conformer increases and the structure is energetically unfavorable.

The tautomer with proton attached to the imidazole ring is denoted $HisH^+[N^\delta]$. A set of 27 unique conformers was located. Table 6 lists the relative energies, relative zero-point vibrational energies, relative enthalpies, relative free energies, rotational data, and dipole moments for the four most stable conformers of $HisH^+[N^\delta]$. Because the $N^\delta H$ on the imidazole ring can serve as a good H-bond donor, six types of H-bond ($OH\cdots NH_2$, $N^\delta H\cdots NH_2$, $N^\delta H\cdots O{=}C$, $N^\delta H\cdots OH$, $CH_r\cdots NH_2$, and $CH_r\cdots O{=}C$) were found on the basis of the AIM analysis. The $OH\cdots NH_2$, $N^\delta H\cdots NH_2$, $N^\delta H\cdots O{=}C$, and $N^\delta H\cdots OH$ H-bonds are moderately strong with average energies of −8.3, −8.6, −10.2, and −6.3 kcal/mol, respectively. The $CH_r\cdots NH_2$ and $CH_r\cdots O{=}C$ H-bonds are weak with the average energies of −2.2 and −3.0 kcal/mol, respectively. The two most stable conformers are stabilized by the $N^\delta H\cdots NH_2$ H-bond and through the favorable interaction between the amino group and the carboxylic group, while the third most stable conformer is stabilized by the $OH\cdots NH_2$ and $N^\delta H\cdots O{=}C$ H-bonds (Figure 6).

The most stable conformer of $HisH^+[N^\delta]$ is more stable than its $HisH^+[NH_2]$ counterpart by 2.1 kcal/mol in the free energy scale. Consequently, $HisH^+[N^\delta]$ is the dominant product of the protonation process.

Bivalent Cation ($HisH_2^{2+}$). The two protons are respectively attached to the amino group and the imidazole ring. A set of

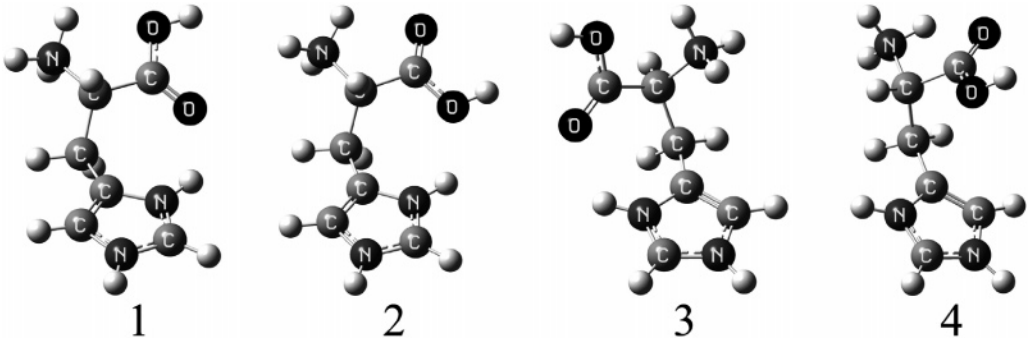

Figure 7. Structures of the four most stable conformers of doubly protonated histidine ion $HisH_2^{2+}$.

TABLE 7: Relative Electronic Energies, Enthalpies, Free Energies, Rotational Data, and Dipole Moments for the Four Most Stable Conformers of Doubly Protonated Histidine in the Gas Phase[a]

	relative energy					rotational constant			
conformer	B1	B2	M	relative enthalpy	relative free energy	A	B	C	dipole moment (D)
1	0.00	0.00	0.00	0.00	0.00	2.393	0.641	0.525	5.29
2	3.03	2.68	2.64	2.62	2.36	2.381	0.634	0.517	4.72
3	3.76	3.67	3.34	3.63	3.71	2.074	0.708	0.598	6.01
4	5.19	3.76	3.67	3.67	2.73	2.182	0.659	0.586	5.20

[a] See footnote *a* of Table 1.

17 conformers was located, and their energies vary by about 24 kcal/mol at the BLYP/6-311+G(2df,p) level. Table 7 summarizes the relative energies, rotational constants, dipole moments, and thermodynamic data for the four most stable conformers. Due to the repulsive Coulomb interaction in the bivalent cation, the most stable conformers adopt the structures in which the carboxyl group lies between the ammonium and imidazole ring (Figure 7). The COOH group is the only H-bond acceptor in the bivalent cation. Four types of H-bond ($N^{\epsilon}H\cdots O{=}C$, $N^{\epsilon}H\cdots OH$, $NH_3^+\cdots O{=}C$, and $CH_r\cdots O{=}C$) were identified in the 17 conformers by the AIM analysis. The average energies for $N^{\epsilon}H\cdots O{=}C$, $N^{\epsilon}H\cdots OH$, $NH_3^+\cdots O{=}C$, and $CH_r\cdots O{=}C$ H-bonds are −4.5, −2.8, −7.3, and −2.2 kcal/mol, respectively.

Brief Comment on the Hydrogen Bond and the Role of Imidazole Ring. It is clear from the above analysis that the intramolecular H-bond is a key factor in the relative stability of histidine and its related ions. Establishing an H-bond requires the donation of a proton toward the nonbonding electron pair of a heteroatom. Many proton donors and proton acceptors exist in each neutral, deprotonated, and protonated species, resulting in the formation of various intramolecular hydrogen bonds. To benefit from the intramolecular interaction, the protonation or deprotonation process typically involves massive and characteristic conformational changes, as observed above.

As discussed in the previous sections, the imidazole ring is an excellent donor as well as a good acceptor in the canonical neural, deprotonated, and protonated species. Both the protonation and deprotonation of histidine occur on the imidazole ring. This property of histidine is unique and characteristically different from any other single amino acid, where either protonation or deprotonation or both take place mainly in the backbone. Due to this special property and that the imidazole ring is preserved with the peptide chain formation, the imidazole ring in histidine can provide ligand to bind free proton and metal ions such Fe^{2+} in heme as well as act as a donor to form the intermolecular interaction and salt bridge.[59] The capability enables histidine residues to serve critical functional roles, acting either as nucleophiles or as electrophiles. The oxygen transporting function of hemoglobin can be realized by altering histidine residue protonation on N^{δ} of the imidazole ring in the *T* vs *R* state.[37] The protonation state and hydrogen bonding of the histidine residues in HasASM may be responsible for the heme capture and release processes.[60]

Characteristic IR Spectra. Figure 8 shows the simulated IR spectra of the most stable conformers of neutral, protonated, and deprotonated histidine. The IR spectra of imidazole are also shown for comparison. The IR spectra for the corresponding tautomers of histidine species can be found in the Supporting Information. Naturally, there are some characteristic differences in the IR spectra of different species. For example, the characteristic peak for the imidazole $N^{\epsilon}H$ wag at 496 cm^{-1} is preserved in His[$N^{\epsilon}H$] (though shifted to 514 cm^{-1}) but is absent in His[$N^{\delta}H$]. This vibrational mode can be used for the gas-phase IR measurement to distinguish the two tautomers unambiguously.

The most distinct feature of the $HisH^+[N^{\delta}]$ spectrum is a high-intensity band at about 3000 cm^{-1} due to the $\upsilon(N^{\delta}H^+)$ stretching vibration. Due to the strong $N^{\delta}H\cdots NH_2$ H-bond, the $\upsilon(N^{\delta}H^+)$ stretching frequency is red-shifted by about 490 cm^{-1} relative to the $N^{\epsilon}-H$ stretching vibration. If the amino group were protonated, one would observe a strong band at about 2570 cm^{-1} due to the N−H symmetric stretching vibration of the NH_3^+ group and red-shifted significantly by the strong $NH_3^+\cdots N^{\delta}$ H-bond, similar to that observed for the zwitterionic L-tryptophan.[61] For the most stable deprotonated histidine $His^-[N^{\epsilon}H]$, there is a very strong band at 2176 cm^{-1} due to the carboxyl O−H stretching vibration and it is red-shifted greatly due to the $OH\cdots N^{\delta}$ H-bonding interaction. This band is absent in His^-[COOH]. However, there is a $N^{\epsilon}H$ wag band at 441 cm^{-1} in His^-[COOH]. Therefore, both the protonation and deprotonation forms of gaseous histidine and their tautomers have their characteristic vibrational modes and can be determined by IR measurements.

Gas-Phase Thermodynamic Properties of Histidine and Related Ions. Calculated proton affinity, proton dissociation energy, and gas-phase basicity and acidity for the histidine and its related ions through possible reaction paths (Scheme 1) are listed in Table 8. As shown in Table 8, the calculated PDE and GA of reaction A and PA and GB of reaction C at the B3LYP/6-311++G** or B3LYP/6-311+G(2df,p) level are both in excellent agreement with the experimental data.[7,25] These results

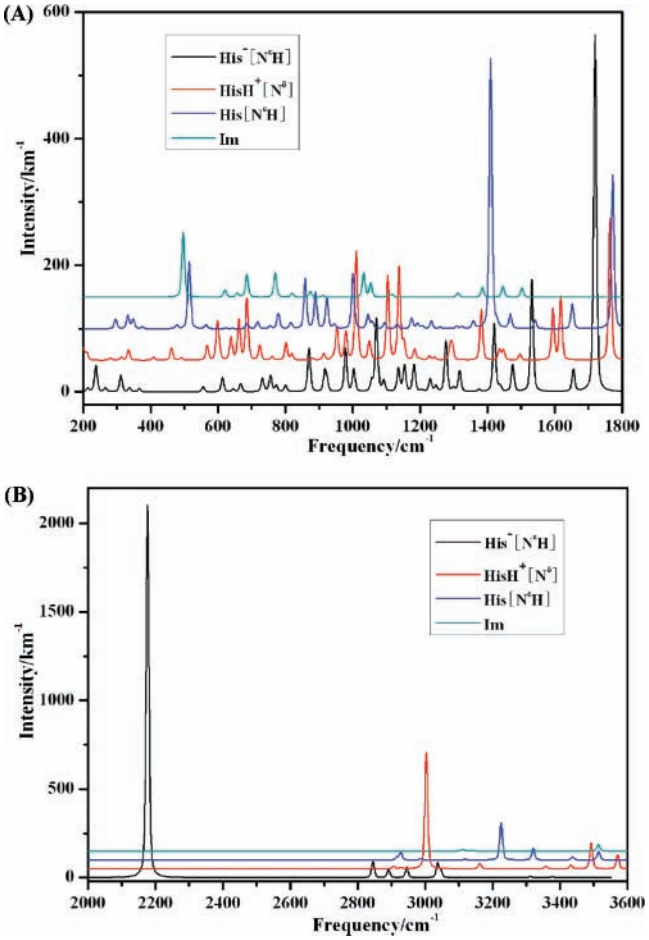

Figure 8. Simulated IR spectra of the most stable conformers of imidazole and neutral, deprotoated, and protonated histidine species. The IR bands are Gaussians with the full width at half-maximum (fwhm) of 10 cm^{-1}: (A) fingerprint region; (B) high-frequency vibration region.

are consistent with the energy ordering of His^-[COOH] and $His^-[N^{\epsilon}H]$ and that of $HisH^+[NH_2]$ and $HisH^+[N^{\delta}]$ discussed above and show clearly that the deprotonation and protonation processes of gaseous histidine molecule both take place on the imidazole ring (i.e., the reaction paths A and C in Scheme 1, respectively). The nature of the proton-transfer processes of the imidazole ring through its two side chain nitrogen atoms enables histidine residues the key role to serve as a general acid or base in different biological processes such as that observed in refs 62 and 63.

As shown in Table 8, the B3LYP/6-311G* results for PDE and GA are higher than the B3LYP/6-311++G** or B3LYP/6-311+G(2df,p) results by about 5 kcal/mol for reactions A and B and by 9 kcal/mol for reactions E and F. This indicates that diffuse functions and polarization functions are important for providing accurate results about anionic species. On the contrary, the augmentation of diffuse and polarization functions has a small influence on the calculation of cationic species and the B3LYP/6-311G* results for PA and GB are close to that of B3LYP/6-311++G** and B3LYP/6-311+G(2df,p) calculations. It appears that the B3LYP method with a medium-size basis set including diffuse and polarization functions (such as 6-311++G** and 6-311+G(2df,p)) is suitable for calculating gas-phase thermodynamic properties for amino acids and their derivatives. However, the results at the MP2/6-311+G(2df,p) level as shown in Table 8 are much less satisfactory.

It is worthy noting that the GA/GB results have little change when the conformational equilibrium is considered, consistent with the finding of Chung-Phillips for glycine.[14] Therefore, the properties of the most stable species are often representative of the full equilibrium ensemble.

Vertical Ionization eEnergy and Electron Affinity. Ionization energies (IEs) and electronic affinities (EAs) are important for understanding the charge transfer, electrophilicity, and reactivity redox potential of biological molecules. Table 9 shows the calculated vertical IEs of the four most stable conformers of gas-phase histidine tautomers and their protonated and deprotonated species. The vertical IEs of histidine are conformation-dependent, but the variation is limited for the equilibrium population with the observable IE of about 8.5 eV and characteristically different from that of phenylalanine.[54,64,65] By the same computational method, the vertical IEs of gaseous imidazole and 4-methylimidazole molecules are found to be 8.96 and 8.48 eV, respectively. Therefore, the IEs of histidine are close to that of 4-methylimidazole instead of imidazole. As noted in passing, our calculations show that substituting the proton with Na^+ on the imidazole of histidine reduces the vertical IE by almost 2 eV. Understandably, metal ion substitutions are very effective in reducing the redox potential of a biological molecule.

It may be pointed out that our vertical IE result of 8.52 eV for the most stable conformer of $His[N^{\delta}H]$ is quite different from the former result of 7.76 eV by the outer-valence-Green's-functions (OVGF) method.[66] On the other hand, our VIE result of 8.43 eV for the most stable conformer of $His[N^{\epsilon}H]$ is in good agreement with the OVGF value of 8.34 eV. The inconsistent agreement between our IE results and the OVGF IE results is caused mainly by the incomplete conformational search of the previous study.

The adiabatic ionization energies of histidine, 2-methylimidazole (or 4-methylimidazole) and the vertical ionization energies of 1-methylimidazole and 2-methylimidazole were experimentally[67,68] determined to be 8.20, 8.50, 8.66, and 8.50 eV, respectively. The corresponding computational results we obtain are 7.92 (for $His[N^{\epsilon}H]$), 8.25, 8.69, and 8.47 eV, respectively. The measured and the calculated values are in agreement within a range of 0.3 eV, as also observed previously.[64] To avoid arriving at an incorrect conclusion, it is important to bear in mind the theoretical error bar of 0.3 eV. For example, the theoretical adiabatic IE of the most stable $His[N^{\delta}H]$ conformer is 8.17 eV and is in better agreement with the experiment than that of $His[N^{\epsilon}H]$. However, the global minimum is of the tautomeric form of $His[N^{\epsilon}H]$ instead of $His[N^{\delta}H]$ as determined by the relative conformational energies and the PDE and GB results discussed above.

The observable vertical IE of deprotonated histidine is 3.78 eV for the most stable $His^-[N^{\epsilon}H]$ conformer. The vertical IEs of deprotonated imidazole, formic acid, and acetic acid anion are respectively 2.75, 3.61, and 3.76 eV according to our calculations. Clearly, the ionization energy of deprotonated histidine is best represented by deprotonated acetic acid instead of deprotonated imidazole. This unexpected correspondence is due to that a significant portion of the electron is transferred from the imidazolate ring to the carboxyl in deprotonated histidine.

The vertical IEs of His^{2-} are about −0.2 eV. Negative ionization energies of dianions were observed experimentally before.[69,70] The conformers of His^{2-} are stabilized by the repulsive Coulomb potential barrier between the negative charge centers of carboxylic ion and imidazole ion. The vertical IEs of protonated and doubly protonated histidines are 13.1 and 17.4 eV, respectively.

TABLE 8: Theoretical Proton Affinity/Proton Dissociation Energy and Gas-Phase Basicity/Acidity for Gaseous Histidine[a]

	proton dissociation energy					gas-phase acidity					
reaction	theory				expt[f]	theory					expt[f]
A	338.0[b]	333.1[c]	333.6[d]	327.0[e]	331(3.1)	330.8[b]	326.0[c]	326.4[d]	319.8[e]	326.8[g]	324.1(3.1)
B	346.7	341.5	341.7	339.4		338.9	333.6	333.9	331.5	333.5	
E	423.3	414.0	414.7	414.5		415.0	405.8	406.5	406.2	406.1	
F	414.6	405.7	406.6	402.1		407.0	398.1	399.0	394.5	399.4	
	proton affinity					gas-phase basicity					
reaction	theory				expt[f]	theory					expt[f]
C	237.4[b]	235.0[c]	235.3[d]	231.2[e]	236.1	229.8[b]	227.3[c]	227.6[d]	223.5[e]	227.8[g]	227.1
D	236.6	233.2	233.2	230.8		228.9	225.4	225.5	222.8	225.3	
G	140.8	138.7	138.6	134.9		133.3	131.3	131.2	127.5	130.6	
H	141.6	140.5	140.7	135.3		134.2	133.2	133.3	128.2	133.1	

[a] All energies are in kilocalories per mole. All the thermodynamic data correspond to the reference state of 1 atm, 298 K. Only the most stable conformers were considered for the reactions in the b, c, d, and e columns. [b] Results for the electronic energies obtained at the B3LYP/6-311G* level. [c] Results for the electronic energies obtained at the B3LYP/6-311++G** level. [d] Results for the electronic energies obtained at the B3LYP/6-311+G(2df,p). [e] Results for the electronic energies were obtained at the MP2/6-311+G(2df,p) level. [f] Experimental data were taken from NIST.[25] [g] Results at the B3LYP/6-311+G(2df,p) level with conformer population-averaged free energies.

TABLE 9: Vertical Ionization Energies (eV) of the Four Most Stable Conformers of Histidine and Related Species

conformer	His[N$^{\epsilon}$H]	His[N$^{\delta}$H]	His$^-$[N$^{\epsilon}$H]	His$^-$[COOH]	His^{2-}	HisH$^+$[N$^{\delta}$]	HisH$^+$[NH$_2$]	HisH$_2^{2+}$
1	8.43	8.52	3.78	3.60	−0.25	13.09	12.60	17.37
2	8.58	8.26	3.35	3.67	−0.18	13.39	12.58	17.48
3	8.56	8.14	3.29	3.50	−0.17	13.43	12.57	17.56
4	8.60	8.25	3.23	3.59	−0.32	12.88	12.55	17.22

TABLE 10: Vertical Electronic Affinities (eV) of the Four Most Stable Conformers of Histidine and Related Species[a]

conformer	His[N$^{\epsilon}$H]	His[N$^{\delta}$H]	His$^-$[N$^{\epsilon}$H]	His$^-$[COOH]	His^{2-}	HisH$^+$[N$^{\delta}$]	HisH$^+$[NH$_2$]	HisH$_2^{2+}$
1	−0.53 (−0.31)	−0.15 (−0.06)	−3.58 (−3.52)	−3.12 (−3.04)	−6.62 (−6.57)	3.44 (4.00)	3.17 (3.51)	7.44(8.08)
2	−0.48	−0.10	−3.58	−3.07	−6.58	3.42	3.35	7.40
3	−0.39	−0.24	−3.70	−3.14	−6.51	3.41	3.33	7.64
4	−0.50	−0.23	−3.37	−3.11	−6.58	3.38	3.42	7.39

[a] Numbers in parentheses are the adiabatic electronic affinities.

TABLE 11: Excitation Energies ΔE (eV) and Dipole Transition Oscillator Strengths $f(r)$ of Imidazole, Imidazolium, 4-Methylimidazole, 5-Methylimidazole, and Methylimidazolium

	Im		ImH$^+$		4-MeIm		5-MeIm		MeImH$^+$	
transition state	ΔE	$f(r)$	ΔE	$f(r)$	ΔE	$f(r)$	ΔE	$f(r)$	ΔE	$f(r)$
S0−S1	5.40	0.0004	6.26	0.1464	5.18	0.0000	5.11	0.0014	5.90	0.1533
S0−S2	6.28	0.0262	7.18	0.0000	5.84	0.0055	5.82	0.0035	6.82	0.0006
S0−S3	6.44	0.0023	7.89	0.0000	5.98	0.1206	6.10	0.1726	7.27	0.109
expt	5.69 and 6.20[a]		6.08[b]							

[a] References 76 and 77. [b] Reference 76

TABLE 12: Transitions and Weights of Excited Configurations for the Three Lowest UV Excitations of Imidazole, Imidazolium, 4-Methylimidazole, 5-Methylimidazole, and Methylimidazolium

		Im		ImH$^+$		4-MeIm		5-MeIm		MeImH$^+$	
state	CSF[a]	T[b]	W[c]	T[b]	W[c]	T[b]	W[c]	T[b]	W[c]	T[b]	W[c]
S1	H-1→L+1			$\pi\pi^*$	95					$\pi\pi^*$	3
	H→L	$\pi\pi^*$	100	$\pi\pi^*$	5	$\pi\pi^*$	100	$\pi\pi^*$	100	$\pi\pi^*$	97
S2	H→L+2	$\pi\pi^*$	100	$\pi\sigma^*$	100	$\pi\pi^*$	100	$\pi\sigma^*$	100	$\pi\sigma^*$	100
S3	H-1→L									$\pi\pi^*$	22
	H-1→L+1	Nσ^*	100								
	H→L+1					$\pi\sigma^*$	92	$\pi\sigma^*$	74	$\pi\pi^*$	78
	H→L+3			$\pi\sigma^*$	100			$\pi\pi^*$	26		
	H→L+7					$\pi\sigma^*$	8				

[a] Configuration state functions. H = HOMO, L = LUMO. [b] Type of orbital transition. [c] Weights of excited configurations (%).

Table 10 shows the vertical EAs for the four most stable conformers of gas-phase histidine tautomers and their protonated and deprotonated species. The EAs of canonical neutral histidine are negative, with absolute value smaller than that of imidazole (the theoretical vertical and adiabatic EAs for imidazole are −0.74 and −0.71 eV, respectively). For comparison, the experimental EAs for indole,[71] naphthalene,[72] benzene,[72] and anthracene[73] are −1.03 meV, −0.19 eV, −1.12 eV, and 0.53 eV, respectively.

3.2. Absorption Spectra and Characterizations of the Excited States. *Accuracy of the Computational Method.* We began the excited-state study with verifying the accuracy of the TDDFT method for aromatic biomolecules. The S_0-S_1 transition energy of tryptophan is predicted to be 4.50 eV at the B3LYP/

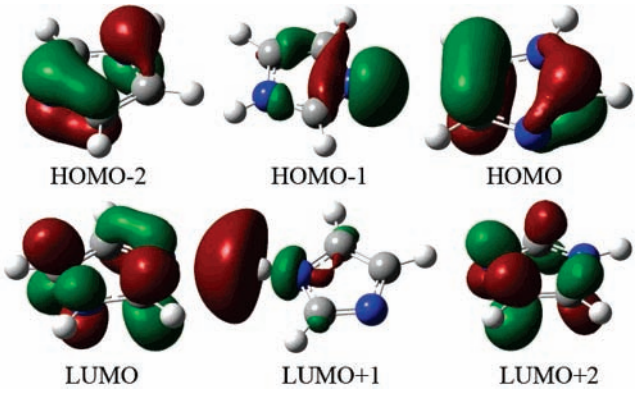

Figure 9. Representative orbitals of imidazole.

6-311+G(2df,p) level, in good agreement with the experimental value of 4.32 eV.[28,32] For the gas-phase indole molecule we predict the two weak low-lying $\pi-\pi^*$ valence singlet transitions, L_b and L_a, at 4.62 and 4.84 eV, in reasonable agreement with the experimental results of 4.37 and 4.77 eV,[74,75] respectively. We expect the TDDFT/B3LYP/6-311+G(2df,p) method to give the excitation energies with an accuracy of about 0.25 eV.

Electronic Spectra of Imidazole, iImidazolium, 4-Methylimidazole, 5-Methylimidazole, and Methylimidazolium. Comparing the spectra of imidazole (Im), imidazolium (ImH^+), 4-methylimidazole (4-MeIm), 5-methylimidazole (5-MeIm), and methylimidazolium ($MeImH^+$) is helpful for discussing the effect of side chain substitution on the electronic spectra. Table 11 compiles the calculated excitation energies and dipole transition oscillator strengths of Im, ImH^+, 4-MeIm, 5-MeIm, and $MeImH^+$ in the gas phase. Table 12 summarizes the structures of the TDDFT wave functions for the three lowest excited transitions of Im, ImH^+, 4-MeIm, 5-MeIm, and $MeImH^+$.

The first two $\pi-\pi^*$ transitions of Im at 5.40 (229 nm) and 6.28 eV (198 nm) with weak oscillator strengths are in good agreement with the experimental values if they are the detected transitions.[76,77] The participating orbitals include the n orbital (HOMO-1) by the unprotonated N lone pair and two π orbitals, π_1 (HOMO) and π_2 (HOMO-2), that are contributed mainly from C and N atoms (Figure 9). The three lowest unfilled orbitals correspond to two π^* (LUMO and LUMO+2) and σ^*_{NH} orbitals, somewhat different from the results at the CNDO/S and INDO/S levels.[78,79] The S_0-S_1 and S_0-S_2 excitations are entirely due to the $\pi_1-\pi_1^*$ and $\pi_1-\pi_2^*$ transitions. The S_0-S_3 transition is entirely due to the $n-\sigma^*_{NH}$ orbital excitation. Notice that the spectra may be red-shifted by about 10 nm due to solvent effect as indicated by the experimental spectra of adentine (an absorption peak at 252 nm in the gas phase is shifted to 260 nm in aqueous solution).[80,81]

The lowest $\pi-\pi^*$ transition of ImH^+ is 6.26 eV with a rather strong oscillator strength of 0.1464. The original first $\pi-\pi^*$ transition is blue-shifted by 0.86 eV (30 nm) due to protonation. The $\pi-\pi^*$ transition involves the HOMO-1→LUMO+1 (weight 95%) and HOMO→LUMO (weight 5%) excitations. The spectrum for ImH^+ is relatively simple due to its symmetry of C_{2v}. The $\pi-\sigma^*$ transitions, being symmetry-forbidden, have zero oscillator strength and no contribution to the resonance Raman spectrum.

Methyl substitutions also bring changes in the excited transitions of the imidazole ring. Depending on the transitions, methylation induces a spectral red shift of 0.2−0.4 eV, similar to the experimental finding for the DNA base guanine.[82] The observed faster degradation of 4-MeImH than that of ImH is attributable to the electron-donating effect of the methyl substituent, which enhances the radical reactivity.[83] Methylation sites have little influence on the first two excitation energies. Methylation increases the dipole oscillator strength of the S_0-S_3 transition, and the transition is changed as HOMO→LUMO+1 ($\pi-\sigma^*$, 92%) and HOMO→LUMO+7 ($\pi-\sigma^*$, 8%) on 4-MeIm and HOMO→LUMO+1 ($\pi-\sigma^*$, 74%) and HOMO→LUMO+3 ($\pi-\pi^*$, 26%) on 5-MeIm. Methylation of ImH^+ destroys the C_{2v} symmetry and makes the S_0-S_2 and S_0-S_3 transitions permitted.

Electronic Spectra of Histidine His[N$^\epsilon$H] and Its tTautomer His[N$^\delta$H]. The excitation energies and transition dipole moments for the most stable conformers of His[N$^\epsilon$H], His[N$^\delta$H], and protonated species are shown in Table 13 (the corresponding results for the second most stable conformers can be found in the Supporting Information for comparison). Table 14 summarizes the structure of the wave functions for the three lowest excitations of histidine, tautomer, and its protonation species. The molecular structure of histidine is similar to that of methylimidazole; however, the electronic spectra are complicated due to the carboxylic and amino groups. The valence orbitals include n_{NO} orbital (HOMO-1), mainly by the O and N lone pair of carboxylic and amino group, and π orbital (HOMO) on the imidazole ring. The three unfilled orbitals are two π^* orbitals contributed from the imidazole ring and the carboxylic group, and an n* orbital of N lone pairs on the imidazole ring. All excited transitions of neutral histidine have very low dipole transition oscillator strengths, explaining the weakness of histidine UVRR bands.[76] The S_0-S_1 transition of histidine at 5.37 eV (231 nm) is a mixed $\pi\pi^*/n\pi^*$ transition (see the orbital plot in Figure 10). The excitation energies vary in the range of 0.1−0.3 eV for the two most stable conformers due to different intramolecular hydrogen bonding.

The NH tautomerism changes the orbital energies and the transition modes. The main valence and unfilled orbitals include two π orbitals and two π^* orbitals (HOMO-3, HOMO, LUMO+1, and LUMO+2) from the imidazole ring, two n orbitals (HOMO-2 and HOMO-1) respectively from the O in carboxylic and N in the amino group and N of the imidazole ring, and a π orbital (HOMO) from the carboxylic group (see Figure S2 of the Supporting Information). The S_0-S_1 transition of the histidine tautomer is red-shifted 0.5 eV relative to that of histidine S_0-S_1 transition. The tautomer S_0-S_1 transition is a pure HOMO→LUMO excitation. This S_0-S_1 excitation is a charge transfer from the imidazole ring to the carboxylic group. The S_0-S_2 and S_0-S_3 transitions are both mixed $n\pi^*/\pi\pi^*$ transitions. The HOMO-1 (n_N orbital) has no contribution to the three lowest excited transitions.

Electronic Spectra of Protonated Histidine HisH$^+$[N$^\delta$], HisH$^+$[NH$_2$], and HisH$_2^{2+}$. As shown in Table 14, the main valence and unoccupied orbitals for UV excitation of $HisH^+$-[N$^\delta$] are a π (HOMO-2) and two π^* orbitals (LUMO and LUMO+1) from the imidazolium ring, two n orbitals (HOMO-1 and HOMO) respectively from the O of the carboxylic group and N of the amino group, and π^* orbital (LUMO+2) from the carboxylic group (Figure 11). The S_0-S_1 excitation of $HisH^+$[N$^\delta$] at 5.45 eV is mainly an $n\pi^*$ transition. The charge transfers from the N lone pair of the amino group to the imidazolium ring. The S_0-S_2 and S_0-S_3 excitations are charge-transfer mainly from the O lone pair of the carboxylic group to the imidazolium ring. These $HisH^+$[N$^\delta$] excitations provide multiion dissociative channels different from that of $HisH^+$-[NH_2] on far-UV excitation. A charge transfer on the S_0-S_1 transition of $HisH^+$[N$^\delta$] is to produce a hypervalent radical $ImH-C_\beta H_2-C_\alpha H(COOH)-NH_2^+$ with the corresponding ion

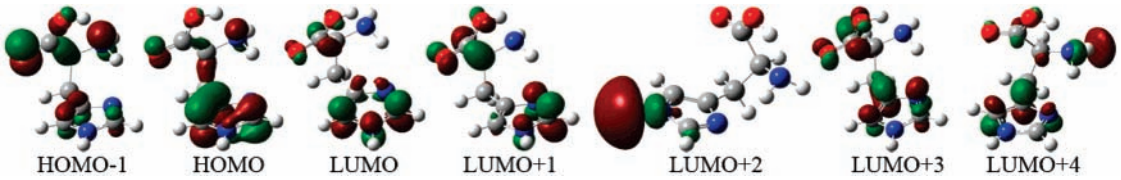

Figure 10. Representative orbitals of the most stable conformer of histidine His[N$^{\epsilon}$H].

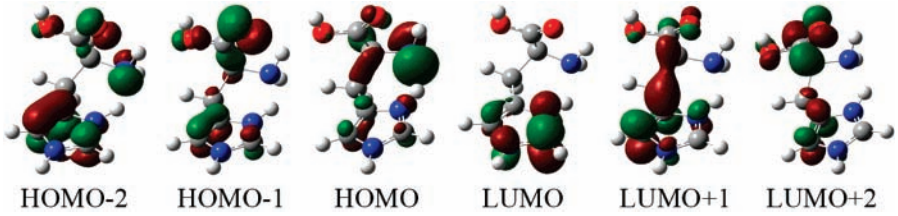

Figure 11. Representative orbitals of the most stable conformer of protonation histidine HisH$^+$[N$^{\delta}$].

TABLE 13: UV Excitation Energies (eV) and Dipole Transition Oscillator Strengths of the Most Stable Conformers of Histidine, Histidine Tautomer, and Protonated and Sodium Ion Binding Histidines

state	His[N$^{\epsilon}$H]	His[N$^{\delta}$H]	HisH$^+$[N$^{\delta}$]	HisH$^+$[NH$_2$]	HisH$_2^{2+}$	Na$^+$(His)
S1	5.37/0.0050	4.85/0.0128	5.45/0.0065	5.28/0.0077	5.63/0.0018	5.04/0.0008
S2	5.44/0.0000	5.47/0.0193	5.67/0.0167	5.73/0.0128	5.80/0.0007	5.49/0.0060
S3	5.69/0.0210	5.52/0.0135	5.82/0.0092	5.94/0.0007	6.26/0.1579	5.91/0.0020

TABLE 14: Transitions and Weights of Excited Configurations for the Three Lowest UV Excitations of the Most Stable Conformer of Histidine, Histidine Tautomer, and Protonated Histidine Species

		histidine		tautomer		HisH$^+$[N$^{\delta}$]		HisH$^+$[NH$_2$]		HisH$_2^{2+}$	
state	CSF[a]	T[b]	W[c]	T[b]	W[c]	T[b]	W[c]	T[b]	W[c]	T[b]	W[c]
S1	H-2→L					$\pi\pi^*$	5				
	H-1→L	nπ^*	16			nπ^*	9			nπ^*	4
	H-1→L+1	nπ^*	11								
	H-1→L+3	nπ^*	5								
	H-1→L+4	nσ^*	3								
	H→L	$\pi\pi^*$	65	$\pi\pi^*$	100	nπ^*	86	$\pi\pi^*$	100	$\pi\pi^*$	96
S2	H-3→L			$\pi\pi^*$	6						
	H-2→L			nπ^*	45	$\pi\pi^*$	7				
	H-2→L+1			nπ^*	11						
	H-2→L+2					$\pi\pi^*$	2				
	H-1→L	nπ^*	17			nπ^*	69			nπ^*	88
	H-1→L+1					nπ^*	6				
	H-1→L+2					nπ^*	11			nπ^*	4
	H-1→L+3	nπ^*	3							nπ^*	3
	H→L	$\pi\pi^*$	12			nπ^*	5			$\pi\pi^*$	5
	H→L+1	$\pi\pi^*$	68	$\pi\pi^*$	38			$\pi\sigma^*$	100		
S3	H-3→L			$\pi\pi^*$	4			nπ^*	42		
	H-2→L			nπ^*	25			nπ^*	40		
	H-2→L+1			nπ^*	4	$\pi\pi^*$	6				
	H-2→L+2					$\pi\pi^*$	7				
	H-1→L	nπ^*	18			nπ^*	23	$\pi\pi^*$	18		
	H-1→L+1	nπ^*	11			nπ^*	33				
	H-1→L+2					nπ^*	31				
	H-1→L+3	nπ^*	6								
	H-1→L+4	nσ^*	3								
	H→L	$\pi\pi^*$	27								
	H→L+1	$\pi\pi^*$	35	$\pi\pi^*$	65					$\pi\pi^*$	100
	H→L+2			$\pi\pi^*$	2						

[a] Configuration state functions. H = HOMO, L = LUMO. [b] Type of orbital transition. [c] Weights of excited configurations (%).

fragments upon dissociation, while the S_0-S_2 and S_0-S_3 excitations produce a radical Im$H-C_{\beta}H_2-C_{\alpha}H(NH_2)-(COOH)^+$ and the corresponding ion fragments. The UV excitations of HisH$^+$[N$^{\delta}$] are characteristically different from that of protonated tryptophan with which the fragmentation started with the dissociation of an H atom.[33]

The excitation modes for HisH$^+$[NH$_2$] are relatively simple. The main valence and unfilled orbitals of HisH$^+$[NH$_2$] include two π orbitals (HOMO-1 and HOMO) from the imidazole ring, two n orbitals (HOMO-3 and HOMO-2) respectively from N of the imidazole ring and the O of the carboxylic group, a π^* orbital (LUMO) from the carboxylic group, and a σ^* orbital (LUMO+1) from the amine NH_3^+ (see Figure S3 of the Supporting Information). The S_0-S_1 excitation, being a $\pi\pi^*$ transition, is a charge transfer from the imidazole ring (HOMO) to the carboxylic group (LUMO). Protonation leads to a red-shift of 0.1 eV on the S_0-S_1 excitation. The S_0-S_2 excitation is a $\pi\sigma^*$ transition. The charge transfers from the imidazole ring (HOMO) to the amine group (LUMO+1), similar to that found in protonated tryptophan in the gas phase[33−35] and in

protein.[84] The S_0-S_3 excitation is a mixed $n\pi^*/\pi\pi^*$ transition. These excited states provide multiplex dissociation channels of protonated histidine on UV excitation. The first excitation at 5.28 eV can be a dissociative state on the carboxylic group, while the second excitation at 5.73 eV is a dissociative state on the amine group.

The electronic spectrum of doubly prontonated histdine ($HisH_2^{2+}$) is also shown in Table 13. The S_0-S_1 transition at 5.63 eV happens between the π orbital (HOMO) of the imidazolium ring and the π^* orbital (LUMO) of the carboxylic group (Figure S4 of the Supporting Information).

The electronic spectrum of the $Na(His)^+$ complex is also calculated and shown in Table 13 for comparison. The Na^+ bonding configuration in the $Na(His)^+$ complex is similar to that for $HisH^+[N^\delta]$. However, the S_0-S_1 transition of the $Na(His)^+$ complex is between the π orbital (HOMO) of the imidazole ring and the π^* orbital (LUMO) of the carboxylic group. The S_0-S_1 transition is red-shifted by 0.3 eV relative to the neutral histidine. The S_0-S_2 transition of $Na(His)^+$ complex transfers charge from Im(π) to Na^+ with an excitation energy of 5.49 eV, coinciding with that observed in the $Cu(Im)_4^+$ complex.[85]

4. Summary

All conformations of histidine, histidine tautomer, and singly and doubly protonated and deprotonated histidines in gas phase have been located by geometry optimizations of all possible trial structures at the B3LYP/6-311G* level of theory initially and followed by the B3LYP/6-311++G** optimization and frequency analysis as well as by B3LYP/6-311+G(2df,p) and MP2/6-311+G(2df,p) calculations. Intramolecular hydrogen bonding interactions of these conformers were analyzed and characterized on the basis of AIM theory. The intramolecular H-bonds are critically important for the relative stabilities of the conformations of histidine and its related ions. The protonation or deprotonation processes induce massive conformational changes involving both the backbone and side chain torsions.

The electron affinities and ionization energies of the most stable conformers of the histidine species are calculated. The proton affinities/proton dissociation energies and gas-phase basicities/acidities of neutral histidine calculated at the B3LYP/6-311++G** or B3LYP/6-311+G(2df,p) level are in excellent agreement with the experimental results. The deprotonation and protonation reaction paths were determined to be both on the imidazole ring. The imidazole ring has a lower acidity and higher basicity than the histidine backbone for the transfer of the proton, ensuring the versatile biological functions of histidine to be preserved in large biomolecules.

The IR spectra of histidine and its protonated and deprotonated species are calculated with their characteristic features pointed out for further experimental verification. The UV spectra of these histidine species are investigated by the TDDFT/B3LYP/6-311+G(2df,p) method. The UV spectra are also distinct and are useful for elucidating the experimental results. For example, the S_0-S_1 transition of histidine tautomer is at 4.85 eV, a red shift of 0.52 eV to that of histidine. Protonation on different sites lead to different transition modes of orbital excitation. The S_0-S_1 excitation of $HisH^+[N^\delta]$ at 5.45 eV transfers charge from the N lone pair of amino group to the imidazolium ring, while the S_0-S_1 excitation of $HisH^+[NH_2]$ at 5.28 eV transfers charge from the imidazole ring to the carboxylic group. The S_0-S_1 excitation of $HisH^+[N^\delta]$ produces a hypervalent radical $ImH-C_\beta H_2-C_\alpha H(COOH)-NH_2^+$, while the S_0-S_2 and S_0-S_3 transitions produce a radical $ImH-C_\beta H_2-C_\alpha H(NH_2)-(COOH)^+$. The existence of these states can exhibit multiplex dissociation channels of protonated histidine and can be inferred indirectly by the relaxation or fragmentation dynamics following photoexcitation. The simulation of these data would allow a better understanding of the excited states of protonated histidine and the fundamental mechanisms involved in the UV fragmentation of biomolecules.

Acknowledgment. Z.L. thanks the National Science Foundation of China (Grant No. 10574114) and the Chinese Academy of Sciences through the Hundred Talent Program for financial support.

Supporting Information Available: UV excitation energies (eV) and dipole transition oscillator strengths of the second most stable conformers of histidine, histidine tautomer, and protonated and histidine species, simulated IR spectra of the most stable conformers of tautomers of neutral, deprotoated, and protonated histidine species, and representative orbitals of the most stable conformers of histidine tautomer $His[N^\delta H]$, protonated histidine tautomer $HisH^+[NH_2]$, and doubly protonated histidine $HisH_2^{2+}$. This material is available free of charge via the Internet at http://pubs.acs.org.

References and Notes

(1) Roth, A.; Breaker, R. R. *Proc. Natl. Acad. Sci. U.S.A.* **1998**, *95*, 6027.
(2) Desfrançois, C.; Carles, S.; Schermann, J. P. *Chem. Rev.* **2000**, *100*, 3943.
(3) Wu, Z.; Fenselau, C. *J. Am. Soc. Mass Spectrom.* **1993**, *3*, 863.
(4) Wu, J.; Lebrilla, C. B. *J. Am. Chem. Soc.* **1993**, *115*, 3270.
(5) McKiernman, J. W.; Beltrame, C. E. A.; Cassady, C. *J. J. Am. Soc. Mass Spectrom.* **1994**, *5*, 718.
(6) Cassady, C. J.; Carr, S. R.; Zhang, K.; Chung-Phillips, A. *J. Org. Chem.* **1995**, *60*, 1704.
(7) Hunter, E. P.; Lias, S. G. *J. Phys. Chem. Ref. Data* **1998**, *27*, 413.
(8) Jensen, F. *J. Am. Chem. Soc.* **1992**, *114*, 9533.
(9) Bliznyuk, A. A.; Schaefer, H. F., III; Amster, I. J. *J. Am. Chem. Soc.* **1993**, *115*, 5149.
(10) Yu, D.; Rauk, A.; Armstrong, D. A. *J. Am. Chem. Soc.* **1995**, *117*, 1789.
(11) Colas, C.; Bouchonnet, S.; Rogalewicz-Gilard, F.; Popot, M. A.; Ohanessian, G. *J. Phys. Chem. A* **2006**, *110*, 7503.
(12) Uggerud, E. *Theor. Chem. Acc.* **1997**, *97*, 313.
(13) Topol, I. A.; Burt, S. K.; Toscano, M.; Russo, N. *J. Mol. Struct. (THEOCHEM)* **1998**, *430*, 41.
(14) Zhang, K.; Chung-Phillips, A. *J. Phys. Chem. A* **1998**, *102*, 3625.
(15) Maksic, Z. B.; Kovacevic, B. *Chem. Phys. Lett.* **1999**, *307*, 497.
(16) Sun, W.; Kinsel, G. R.; Marynick, D. S. *J. Phys. Chem. A* **1999**, *103*, 4113.
(17) Noguera, M.; Rodríguez-Santiago, L.; Sodupe, M.; Bertran, J. *J. Mol. Struc. (THEOCHEM)* **2001**, *537*, 307.
(18) Rak, J.; Skurski, P.; Simons, J.; Gutowski, M. *J. Am. Chem. Soc.* **2001**, *123*, 11695−.
(19) Hudáky, P.; Perczel, A. *J. Phys. Chem. A* **2004**, *108*, 6195.
(20) Zhang, K.; Zimmerman, D. M.; Chung-Phillips, A.; Cassady, C. J. *J. Am. Chem. Soc.* **1993**, *115*, 10812.
(21) Somogyi, A.; Wysocki, V. H.; Mayer, I. *J. Am. Soc. Mass Spectrom.* **1994**, *5*, 704.
(22) Ling, S. L.; Yu, W. B.; Huang, Z. J.; Lin, Z. J.; Harańczyk, M.; Gutowski, M. *J. Phys. Chem. A* **2006**, *110*, 12282.
(23) Bader, R. F. M. *Atoms in Molecules. A Quantum Theory*; Clarendon Press,: Oxford, U.K., 1990.
(24) Popelier, P. L. A. *Atoms in Molecules. An Introduction*; Prentice Hall,: Harlow, U.K., 2000.
(25) *NIST Chemistry Webbook*; NIST Standard Reference Database No. 69; Mallard, W. G., et al., Eds.; National Institute of Standards and Technology: Gaithersburg, MD, March 2003 (http://webbook.nist.gov).
(26) Wetlaufer, D. B. Ultraviolet spectra of proteins and amino acids. In *Advances in Protein Chemistry*; Anfinsen, C. B., Anson, M. L., Bailey, K., Edsall, J. T., Eds.; Academic Press: New York, 1962; Vol. 17.
(27) Demchenko, A. P. *UltraViolet Spectroscopy of Proteins*; Springer-Verlag: Berlin, 1986.

(28) Rizzo, T. R.; Park, Y. D.; Peteanu, L. A.; Levy, D. H. *J. Chem. Phys.* **1986**, *84*, 2534.
(29) Lindinger, A.; Toennies, J. P.; Vilesov, A. F. *J. Chem. Phys.* **1999**, *110*, 1429.
(30) Piuzzi, F.; Dimicoli, I.; Mons, M.; Tardivel, B.; Zhao, Q. *Chem. Phys. Lett.* **2000**, *320*, 282.
(31) Grace, L. I.; Cohen, R.; Dunn, T. M.; Lubman, D. M.; de Vries, M. S. *J. Mol. Spectrosc.* **2002**, *215*, 204.
(32) Snoek, L. C.; Robertson, E. G.; Kroemer, R. T.; Simons, J. P. *Chem. Phys. Lett.* **2000**, *321*, 49.
(33) Kang, H.; Dedonder-Lardeux, C.; Jouvet, C.; Martrenchard, S.; Grégoire, G.; Desfrançois, C.; Schermann, J. P.; Baratc, M.; Fayeton, J. A. *Phys. Chem. Chem. Phys.* **2004**, *6*, 2628.
(34) Nolting, D.; Marian, C.; Weinkauf, R. *Phys. Chem. Chem. Phys.* **2004**, *6*, 2633.
(35) Talbot, F. O.; Tabarin, T.; Antoine, R.; Broyer, M. Dugourd. P. *J. Chem. Phys* **2005**, *122*, 74310.
(36) Boyarkin, O. V.; Mercier, S. R.; Kamariotis, A. Rizzo. T. R. *J. Am. Chem. Soc.* **2006**, *128*, 2816.
(37) Zhao, X.; Wang, D.; Spiro. T. G. *J. Am. Chem. Soc.* **1998**, *120*, 8517.
(38) Zhao, X.; Wang, D.; Spiro, T. G. *Inorg. Chem.* **1998**, *37*, 5414.
(39) Vargek, M.; Zhao, X. J.; Lai, Z. H.; McLendon, G. L.; Spiro, T. G. *Inorg. Chem.* **1999**, *38*, 1372.
(40) Huang, Z.; Yu, W.; Lin. Z. *J. Mol. Struct. (THEOCHEM)* **2006**, *801*, 7.
(41) Stepanian, S. G.; Reva, I. D.; Radchenko, E. D.; Adamowicz, L. *J. Phys. Chem. A* **1999**, *103*, 4404.
(42) Stepanian, S. G.; Reva, I. D.; Radchenko, E. D.; Adamowicz, L. *J. Phys. Chem. A* **1998**, *102*, 4623.
(43) Frisch, M. J.; Trucks, G. W.; Schlegel, H. B.; Scuseria, G. E.; Robb, M. A.; Cheeseman, J. R.; Zakrzewski, V. G.; Montgomery, J. A.; Stratmann, R. E.; Burant, J. C.; Dapprich, S.; Millam, J. M.; Daniels, A. D.; Kudin, K. N.; Strain, M. C.; Farkas, O.; Tomasi, J.; Barone, V.; Cossi, M.; Cammi, R.; Mennucci, B.; Pomelli, C.; Adamo, C.; Clifford, S.; Ochterski, J. Petersson, G. A.; Ayala, P. Y.; Cui, Q.; Morokuma, K.; Malick, D. K.; Rabuck, A. D.; Raghavachari, K.; Foresman, J. B.; Cioslowski, J.; Ortiz, J. V.; Baboul, A. G.; Stefanov, B. B.; Liu, G.; Liashenko, A.; Piskorz, P.; Komaromi, I.; Gomperts, R.; Martin, R. L.; Fox, D. J.; Keith, T.; Al-Laham, M. A.; Peng, C. Y.; Nanayakkara, A.; Challacombe, M.; Gill, P. M. W.; Johnson, B.; Chen, W.; Wong, M. W.; Andres, J. L.; Gonzalez, C.; Head-Gordon, M.; Replogle, E. S.; Pople, J. A. *Gaussian 98*, Revision A.9; Gaussian, Inc.: Pittsburgh, PA, 1998.
(44) Pacios, L. F.; Gálvez, O.; Gómez, P. C. *J. Phys. Chem. A* **2001**, *105*, 5232.
(45) Dobado, J. A.; Martínez-García, H.; Molina, J. M.; Sundberg, M. R. *J. Am. Chem. Soc.* **1999**, *121*, 3156.
(46) Dobado, J. A.; Martínez-García, H.; Molina, J. M.; Sundberg, M. R. *J. Am. Chem. Soc.* **2000**, *122*, 1144.
(47) Espinosa, E.; Molins, E.; Lecomete, C. *Chem. Phys. Lett.* **1998**, *285*, 170.
(48) Custelcean, R.; Jackson, J. E. *Chem. Rev.* **2001**, *101*, 1963.
(49) Alkorta, I.; Rozas, I.; Elguero, J. *Chem. Soc. Rev.* **1998**, *27*, 163.
(50) Sobolewski, A. L.; Domcke, W.; Dedonder-Lardeux, C.; Jouvet, C. *Phys. Chem. Chem. Phys.* **2002**, *4*, 1093.
(51) Dedonder-Lardeux, C.; Jouvet, C.; Perun, S.; Sobolewski, A. *Phys. Chem. Chem. Phys.* **2003**, *5*, 5118.
(52) Scott, A. P.; Radom, L. *J. Phys. Chem.* **1996**, *100*, 16502.
(53) Henry, B.; Tekely, P.; Delpuech, J. J. *J. Am. Chem. Soc.* **2002**, *124*, 2025.
(54) Ivanov, I.; Klein, M. L. *J. Am. Chem. Soc.* **2002**, *124*, 13380.
(55) Kapota, C.; Ohanessian, G. *Phys. Chem. Chem. Phys.* **2005**, *7*, 3744.
(56) Signorini, G. F.; Chelli, R.; Procacci, P.; Schettino, V. *J. Phys. Chem. B* **2004**, *108*, 12252.
(57) Huang, Z.; Yu, W.; Lin, Z. *J. Mol. Struct. (THEOCHEM)* **2006**, *758*, 195.
(58) Kubicki, M.; Borowiak, T.; Dutkiewicz, G.; Souhassou, M.; Jelsch, C.; Lecomte, C. *J. Phys. Chem. B* **2002**, *106*, 3706.
(59) Musafia, B.; Buchner, V.; Arad, D. *J. Mol. Biol.* **1995**, *254*, 761.
(60) Wolff1, N.; Deniau, C.; Létoffé, S.; Simene, C.; Kumar, V.; Stojiljkovic, I.; Wandersman, C.; Delepierre.; Lecroisey, A. *Protein Sci.* **2002**, *11*, 757.
(61) Cao, X.; Fischer, G. *J. Phys. Chem. A* **1999**, *103*, 9995.
(62) Ash, E. L.; Sudmeier, J. L.; Day, R. M.; Vincent, M.; Torchilin, E. V.; Haddad, K. C.; Bradshaw, E. M.; Sanford, D. G.; Bachovchin, W. W. P. *Proc. Natl. Acad. Sci. U.S.A.* **2000**, *97*, 10371.
(63) Nishihira, J.; Tachikawa, H. J. *Theor. Biol.* **1999**, *196*, 513.
(64) Lee, K. T.; Sung, J.; Lee, K. J.; Kim, S. K.; Park, Y. D. *Chem. Phys. Lett.* **2003**, *368*, 262.
(65) Lee, K. T.; Sung, J.; Lee, K. J.; Park, Y. D.; Kim, S. K. *Angew. Chem., Int. Ed.* **2002**, *41*, 4114.
(66) Dehareng, D.; Dive, G. *Int. J. Mol. Sci.* **2004**, *5*, 301.
(67) Wilson, K. R.; Belau, L.; Nicolas, C.; Jimenez-Cruz, Michael.; Leone, S. R.; Ahmeda, M. *Int. J. Mass. Spectrom.* **2006**, *249*−*250*, 155.
(68) Ramsey, B. G. *J. Org. Chem.* **1979**, *44*, 2093.
(69) Wang, L. S.; Wang, X. B. *J. Phys. Chem. A* **2000**, *104*, 1978.
(70) Wang, X. B.; Niu, S. Q.; Yang, X.; Ibrahim, S. K.; Pickett, C. J.; Ichiye, I.; Wang, L. S. *J. Am. Soc. Chem.* **2003**, *125*, 14072.
(71) Carles, S.; Desfrançois, C.; Schermann, J. P. *J. Chem. Phys.* **2000**, *112*, 3726.
(72) Burrow, P. D.; Michejda, J. A.; Jordan, K. D. *J. Chem. Phys.* **1987**, *86*, 9.
(73) Schiedt, J.; Weinkauf, R. *Chem. Phys. Lett.* **1997**, *266*, 201.
(74) Serrano-Andres, L.; Roos, B. O. *J. Am. Chem. Soc.* **1996**, *118*, 185.
(75) Strickland, E. H.; Horwitz, J.; Billups, C. *Biochemistry* **1970**, *25*, 4914.
(76) Caswell, D. S.; Spiro. T. G. *J. Am. Chem. Soc.* **1986**, *108*, 6470.
(77) Markham, L. M.; Mayne, L. C.; Hudson, B. S. *J. Phys. Chem.* **1993**, *97*, 10319.
(78) Del Bene, J.; Jaffẽ, H. H. *J. Chem. Phys.* **1968**, *48*, 4050.
(79) Bernarducci, E.; Bharadwaj, P. K.; Krogh-Jespersen, K.; Potenza, J. A.; Schugar, H. J. *J. Am. Chem. Soc.* **1983**, *105*, 3860.
(80) Clark, L. B. *J. Phys. Chem.* **1990**, *94*, 2873.
(81) Clark, L. B.; Peschel, G. G.; Tinoco, I., Jr. *J. Phys. Chem.* **1965**, *69*, 3615.
(82) Mons, M.; Dimicoli, I.; Piuzzi, F. Tardivel, B.; Elhanine, M. *J. Phys. Chem. A* **2002**, *106*, 5088.
(83) Wu, Q.; Balakrishnan, G.; Pevsner, A.; Spiro, T. G. *J. Phys. Chem. A* **2003**, *107*, 8047.
(84) Callis, P. R.; Vivian, J. T. *Chem. Phys. Lett.* **2003**, *369*, 409.
(85) Bernarducci, E.; Bharadwaj, P. K.; Kfogh-Jespersen, K.; Potenza, J. A.; Schugar, H. J. *J. Am. Chem. Soc.* **1983**, *105*, 3860.